25 March 2002

ELSEVIER

Chemical Physics Letters 355 (2002) 139–146

CHEMICAL PHYSICS LETTERS

www.elsevier.com/locate/cplett

Separation of contributions to the third-order signal: ultrafast frequency-selected vibrational echo experiments on a metalloporphyrin-CO

Qing-Hua Xu, David E. Thompson, K.A. Merchant, M.D. Fayer *

Department of Chemistry, Stanford University, Stanford, CA 94305, USA

Received 2 January 2002; in final form 5 February 2002

Abstract

One-dimensional and frequency-selected vibrational echo experiments on the CO stretching mode of a metalloporphyrin carbonyl compound (model heme) in poly-methylmethacrylate (PMMA) and in 2-methylteterahydrofuran (2-MTHF) are compared. Spectrally resolving the vibrational echo signal and observing the decay at selected wavelengths, permits the independent detection of the 0–1 and 1–2 vibrational level dephasing dynamics, eliminating cross terms and anharmonic beats. In the high temperature 2-MTHF liquid, 0–1 and 1–2 dephasing dynamics are identical within experimental error. The decays are non-exponential, demonstrating that the CO stretching mode absorption spectrum is not a completely homogeneous, motionally narrowed line. © 2002 Elsevier Science B.V. All rights reserved.

1. Introduction

Nonlinear spectroscopic techniques have proven useful in the study of molecular systems because they enable information to be obtained that cannot be extracted from a linear spectrum. Nonlinear methods can involve electro-magnetic radiation frequencies that span the range from the optical to radio frequency, for example, the electronic transition photon echo to the NMR spin echo. Studies of solute–solvent interaction dynamics have shown that the dynamics can occur on the ps and fs time scales [1]. For the study of such fast time scale processes, NMR spin echo studies are limited by their intrinsic NMR time scale. The electronic transition photon echo and other visible optical nonlinear experiments have greatly advanced because of recent developments and applications of ultrashort pulses [2]. However, molecular vibrations that give rise to vibrational progressions in the electronic absorption spectrum complicate resonant nonlinear experiments involving electronic transitions. Intramolecular vibrational modes have significant influence on third-order nonlinear signals [3,4]. The complexity associated with the simultaneous excitation of many vibronic transitions, can make it difficult to analyze the results of ultrafast

* Corresponding author. Fax: +1-650-723-4817.
E-mail address: fayer@fayerlab.stanford.edu (M.D. Fayer).

0009-2614/02/$ - see front matter
PII: S0009-2614(02)00197-5

nonlinear experiments involving electronic transitions [4,5].

The ultrafast infrared vibrational echo experiment [6–17], the vibrational analog of the NMR spin echo and electronic transition photon echo, can overcome the limitations of its two analogs. Recent developments of ultrafast IR pulses have enabled the vibrational echo to probe dynamics on fs time scales. Vibrational echo experiments are providing significant information on liquids [7,9,15–17], glasses [7,9], and proteins [18–23]. Recent advances using two-dimensional (2-D) methods [10–13,15–17], are increasing the utility of the vibrational echo technique.

It is possible to perform a vibrational echo experiment on a single vibrational fundamental if a relatively long (narrow bandwidth) pulse is used [24]. However, the broad spectral bandwidth that is required to generate ultrashort pulses will usually span both 0–1 (fundamental) and 1–2 transitions unless the anharmonicity of the vibration is very large. The excitation involving three levels adds complexity to the vibrational echo signal [12,14,25,26]. In a two-pulse vibrational echo experiment, in which the two pulses are separated by a variable time delay τ, eight different radiation field–matter interaction pathways, represented by the eight double-sided Feynman diagrams in Fig. 1, will contribute to the total vibrational echo signal [27]. Three diagrams are for the positive time delay region, that is, $\tau > 0$ (R_1, R_2 and R_3), three are for the pulse overlap region, $\tau \cong 0$ (R_4, R_5 and R_6), and two are for the negative time delay region, $\tau < 0$ (R_7 and R_8). Only R_1, R_2 and R_3 will contribute to the echo signal when τ is much greater than the pulse duration. Of these three, R_1 and R_2 involve just the 0–1 transition; however, R_3 also involves the 1–2 transition [27]. In a 1-D echo experiment, the interference of the two-level and three-level terms will produce non-exponential decays that can also have anharmonic beats [12,14,25,26] even if the dynamic dephasing of the individual transitions is exponential. If the individual decays are intrinsically non-exponential, then the 1-D signal is virtually impossible to separate into its components. A 2-D vibrational echo experiment, in which the vibrational echo pulse is frequency-resolved, has been used to reveal the

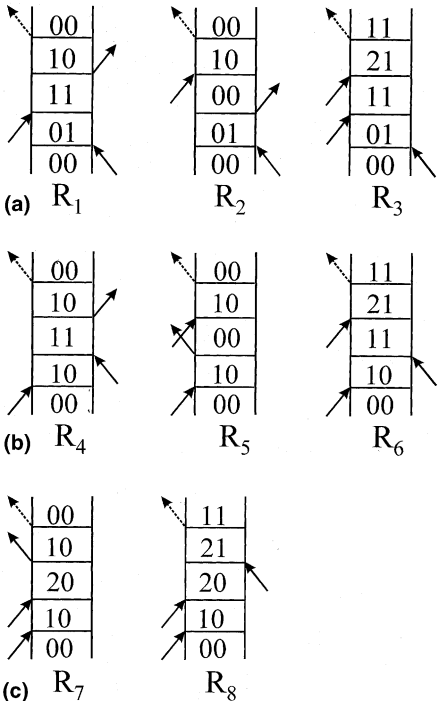

Fig. 1. Double-sided Feynman diagrams for a vibrational echo for a three-level system. Only three levels are involved in a vibrational echo because it is a third-order phenomenon. (a) R_1, R_2 and R_3 are for positive time delay times, time ordering is k_1, k_2, k_3; (b) R_4, R_5 and R_6 for times when the pulses overlap, time ordering is k_2, k_1, k_2; (c) R_7 and R_8 for negative time delay times, time ordering is k_2, k_2, k_1.

nature of the quantum beats and anharmonic beats, and accidental degeneracy beats [14].

In a spectrally resolved 2-D vibrational echo experiment, a 2-D, time–frequency, spectrum is recorded [10,12,13,28]. While full 2-D vibrational echo spectroscopy can provide a variety of types of information that cannot be obtained from a 1-D experiment, in many applications, what is desired is the equivalent of a 1-D experiment, but a 1-D experiment that is free from the complications that arise from the excitation of a multilevel system. In this Letter, it will be demonstrated that by selecting the proper detection wavelength of the vibrational echo signal, which is equivalent to taking appropriated slices through the full 2-D spectrum, it is possible to obtain the ultrafast dephasing dynamics associated with either the 0–1 or 1–2 transitions separately, eliminating cross terms be-

tween the decays and anharmonic beats [25,26]. The signal can thus be modeled as arising from a simple two-level system even though the broad bandwidth associated with the ultrafast infrared pulses excites more than two levels. This technique permits the study of the underlying dynamics of a system without the complications brought on by the anharmonicity or other multi-level effects.

The utility of this technique is demonstrated for the CO stretching mode of a metalloporphyrin carbonyl compound (a model heme), RuTPP-COPy (TPP = 5,10,15,20-tetraphenylporphyrin, Py = pyridine), in two solvents poly-methylmethacrylate (PMMA) and 2-methylteterahydrofuran (2-MTHF). PMMA is a glass at all temperatures studied, while 2-MTHF is a glass forming liquid with its glass transition temperature at 86 K. In contrast to other metal-carbonyl systems that have been studied [8,9,12,24], this system has a single CO mode that is non-degenerate. Therefore, complications produced by quantum beats and those associated with line broadening mechanisms that can arise from degeneracies are avoided. In PMMA, the inhomogeneous line is broad, and there is substantial overlap between the 0–1 and 1–2 transitions, producing strong anharmonic beats in the 1-D vibrational echo decay. These are eliminated through the proper choice of detection wavelength. In 2-MTHF, the absorption line is narrower, and there is little overlap between the 0–1 and 1–2 transitions. No beats are observed in the 1-D spectrum, consistent with theory [12,14]. The vibrational echo decays in the high temperature liquid are non-exponential and virtually identical. In the 2-MTHF solvent, a strong signal at negative time delays is observed because the inhomogeneous line width is narrow.

2. Experimental procedures

The experimental apparatus for the ultrafast infrared vibrational echo has been described in detail previously [12]. Briefly, tunable mid-IR pulses centered at 1948 cm^{-1} with a repetition rate of 1 kHz were generated by an optical parametric amplifier pumped with a regeneratively amplified Ti:Sapphire laser. The bandwidth and pulse duration of the pulses were 90 cm^{-1} (FWHM) and 170 fs (FWHM), and the pulse was nearly transform limited (time-bandwidth product = 0.46). A ZnSe beam splitter was used to create weak (15%, $\mathbf{k_1}$) and strong (85%, $\mathbf{k_2}$) beams. The weak beam was delayed with respect to the strong beam by a stepper-motor translation stage. The beams were crossed and focused at the sample to a spot size of 150 μm. The vibrational echo signal was generated in the phase matched direction $-\mathbf{k_1} + 2\mathbf{k_2}$ and was detected with a liquid nitrogen cooled HgCdTe detector directly (for 1-D signal) or first passed through a monochromator (frequency-selected signal). The resolution of the monochromator was set to 2 cm^{-1}. The pulse energy was ~ 3.5 μJ/pulse (before the beam splitter). Detailed power studies were performed to make sure that there were no higher-order effects and no heating effects.

RuTPPCO, PMMA, methylene chloride (CH_2Cl_2) were purchased from Aldrich and used without further purification. The 2-MTHF (Aldrich) was dried and distilled before use. The RuTPPCOPy/2-MTHF solution was prepared by dissolving the RuTPPCO in 2-MTHF and then adding twofold excess of pyridine into the RuTPPCO solution. Pyridine is the fifth ligand on the Ru. The optical density (OD) of the CO stretching mode in the 200 μm path length sample cell was of 0.1. The PMMA glass film was prepared by mixing PMMA with a RuTPPCOPy/CH_2Cl_2 solution. The solution was spread on a clean glass plate and dried under a closed atmosphere for two days. The sample was then placed under vacuum for a week to remove the remaining solvent. The thickness of the PMMA film sample was 150–200 μm, and the OD was ~0.5 at the absorption maximum. The samples were placed between two CaF_2 windows in a custom gas-tight copper sample cell. The temperature of the sample was controlled with a continuous flow cryostat and monitored with a silicon diode temperature sensor bonded to the front CaF_2 window.

3. Results and discussion

Fig. 2 shows the 1-D vibrational echo data for RuTPPCOPy in PMMA at 80 K. The decay of 1-

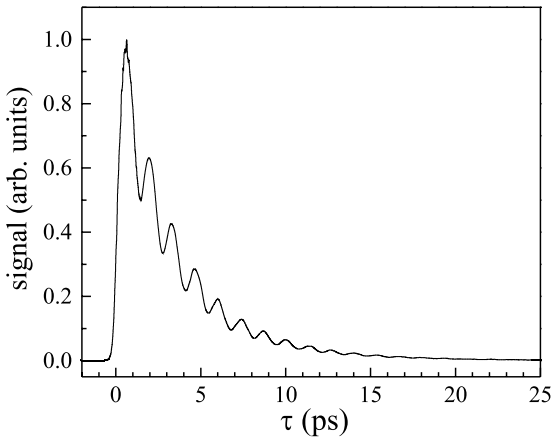

Fig. 2. 1-D vibrational echo decay of RuTPPCOPy in PMMA at 80 K. The bandwidth of the pulse is much larger than the anharmonic shift of the 0–1 and 1–2 transitions. The decay is a tri-exponential with anharmonic beats, that is, beats at the difference in the 0–1 and 1–2 transition frequencies.

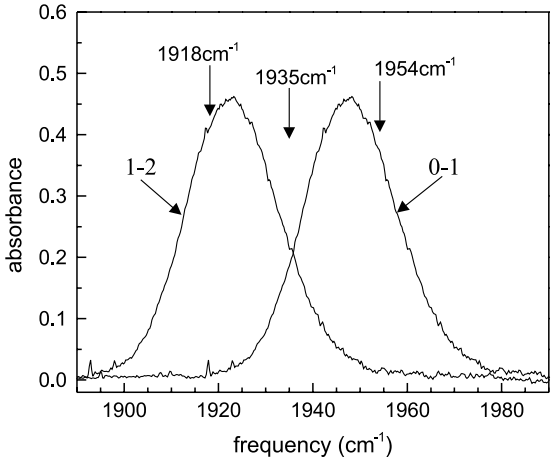

Fig. 3. The absorption spectrum of RuTPPCOPy in PMMA at 80 K labeled 0–1. The curve labeled 1–2 is a model of the 1–2 absorption spectrum obtained by shifting the 0–1 spectrum by the anharmonic shift of 1–2 transition, which was determined from the beat frequency in Fig. 2. The frequencies indicated with arrows correspond to the observations frequencies of the data presented in Fig. 4.

D signal is multi-exponential and is strongly modulated by oscillatory beats. Fig. 3 displays the 0–1 spectrum (fundamental) and 1–2 spectrum (overtone). The 1–2 spectrum was modeled as the 0–1 spectrum shifted by the anharmonicity, which was determined from the beat frequency [25,26]. It is assumed that the line widths are the same for the two transitions. In this system, as shown in Fig. 3, the inhomogeneous broadening ($\sim 22\ \mathrm{cm}^{-1}$) is comparable to the vibrational anharmonicity ($\sim 25\ \mathrm{cm}^{-1}$). When there is spectral overlap of 0–1 and 1–2 transitions, the interference of the R_1/R_2 with R_3 produces a beat at the frequency difference between 0–1 and 1–2 transitions, the anharmonic shift [12,14,25,26]. Such beats are referred to as anharmonic beats [12,14,25,26]. Even if the decays associated with R_1/R_2 and R_3 terms are individually distinct single exponentials, the interference of these terms will cause the total signal to be a tri-exponential with beats. The time constants associated with the individual terms are difficult to resolve, especially when the time constants are similar. If the individual decays are non-exponential and the functional form is not known, then it is virtually impossible to separate the distinct decay components.

The problems associated with the 1-D decay (Fig. 2) can be overcome by performing a frequency-selected vibrational echo. By selecting the proper detection wavelengths, it is possible to obtain the signal corresponding solely to the R_1/R_2 terms (0–1 transition) or to the R_3 term. Fig. 4 displays frequency-selected vibrational echo data for three different detection wavelengths, 1954, 1935 and 1918 cm^{-1} (see Fig. 3). The data in Fig. 4a were taken slightly on blue side of center 0–1 transition (1954 cm^{-1}); the data in Fig. 4b were taken half way between the two transitions (1935 cm^{-1}); and the data in Fig. 4c were taken slightly on red side of the 1–2 transitions (1918 cm^{-1}). In Fig. 4b, the beats are very pronounced with almost 100% modulation depth. In this case, both R_1/R_2 and R_3 terms contribute to the signal, producing strong anharmonic beats at positive delay times. When the blue wavelength is selected (Fig. 4a), only the R_1/R_2 terms contribute to the signal. The decay shown in Fig. 4a (1954 cm^{-1}) is the pure 0–1 transition, two-level vibrational echo decay [14]. When the red wavelength (1935 cm^{-1}, Fig. 4c) is selected, only the R_3 term contributes to the signal. At both wavelengths, the oscillations are virtually eliminated, and the echo decays can be

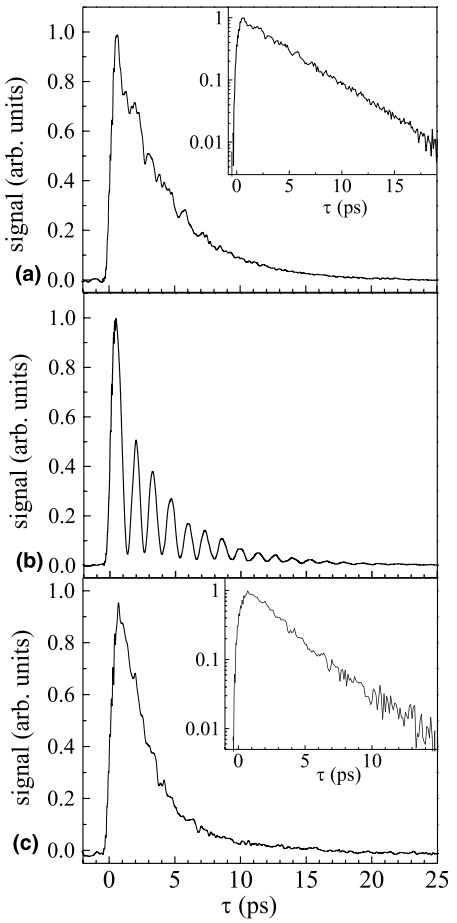

Fig. 4. Frequency-selected vibrational echo decays (slices through the 2-D spectrum) of the CO stretch of RuTPPCOPy in PMMA at 80 K. (a) 1954 cm^{-1}, the 0–1 transition; (b) 1935 cm^{-1}, between the 0–1 and 1–2 transitions; (c) 1918 cm^{-1}, the 1–2 transition. The wavelengths are indicated with arrows in Fig. 3. Almost 100% modulation is seen at 1935 cm^{-1}, where the 0–1 and 1–2 spectra overlap (see Fig. 3). At the other two frequencies, single exponential decays (see insets) are observed.

fit with single exponentials, as shown in the insets.

The decay rate associated with R_3 (Fig. 4c) is faster than that of R_1/R_2 (Fig. 4a). The fact that single exponential echo decay is obtained suggests that the underlying vibrational dynamics can be well separated into homogeneous and inhomogeneous broadening components. The echo decay time of 4 ps for the 0–1 transition (R_1/R_2 terms) gives a dynamic line width of 0.65 cm^{-1} assuming the absorption line is inhomogeneously broadened. This line width is much narrower than the absorption line width (~ 22.8 cm^{-1}), consistent with the assumption that the absorption line is massively inhomogeneously broadened. In this kind of situation, the dynamics can be described in terms of a Bloch description. In the Bloch picture, the decay rates of the signal associated with R_1 and R_2 terms are identical and are denoted by $4\gamma_{01}$, while the decay rate associated with the R_3 term is $(2\gamma_{01} + 2\gamma_{12})$, where γ_{01} and γ_{12} denote the total dephasing rates associated with the 0–1 and 1–2 transitions, respectively. The data demonstrate that the total dephasing rate associated with 1–2 transition is faster than that of 0–1 transition, that is, $\gamma_{01} = 1/(16\text{ ps})$ and $\gamma_{12} = 1/(7\text{ ps})$ at 80 K. The total dephasing process has contributions from both vibrational population relaxation and pure dephasing processes. For a harmonic oscillator, the lifetime of a vibration level is inversely proportional to its quantum number, while the pure dephasing is only dependent on the difference between the quantum numbers of the levels involved. For a system with a small anharmonicity, it is reasonable to assume that the pure dephasing rates associated with 0–1 and 1–2 transitions are very similar (see below). At low temperature, the vibrational population decays of the levels make a significant contribution to the total dephasing [9,26]. Therefore, the difference in the total dephasing rates in the current situation is most likely due to the shorter vibrational lifetime of the $v = 2$ level than that of the $v = 1$ level where v is the vibrational quantum number [26]. The similarity of the pure dephasing rates associated with 0–1 and 1–2 transitions is clearly demonstrated for RuTPPCOPy/2-MTHF at 280 K (Fig. 5c), where the total dephasing rate is dominated by the pure dephasing rate, which is much faster than the corresponding population decay rate.

Fig. 5 displays data taken on RuTPPCOPy/2-MTHF. Fig. 5a shows the 0–1 absorption spectrum and the 1–2 spectrum modeled as the 0–1 spectrum shifted by the anharmonicity. In contrast to RuTPPCOPy/PMMA, the absorption line width is smaller than the anharmonicity; very little spectral overlap exists between the 0–1 and 1–2 transitions. Fig. 5b displays 1-D data taken at

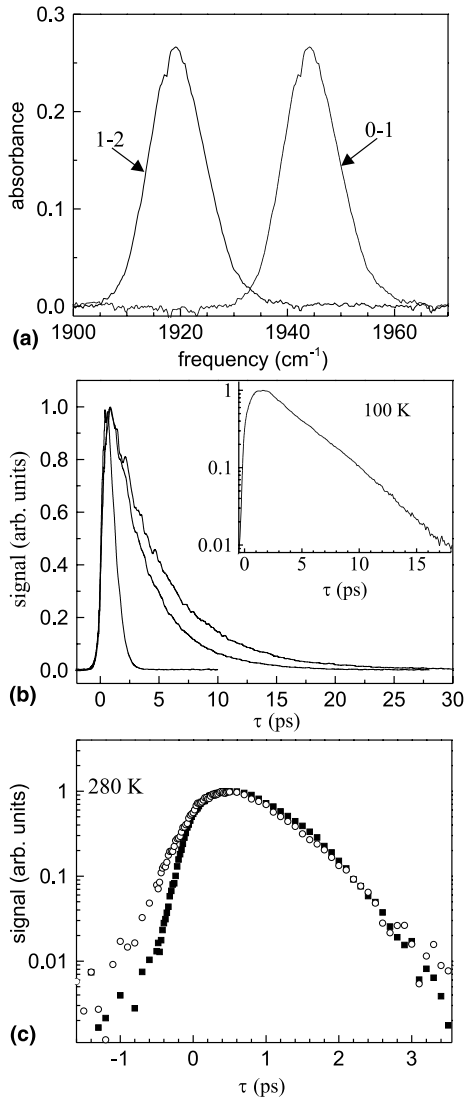

Fig. 5. Data for RuTPPCOPy in 2-MTHF. (a) The absorption spectrum at 100 K labeled 0–1. The curve labeled 1–2 is a model of the 1–2 absorption spectrum obtained by shifting the 0–1 transition by the anharmonic shift. (b) 1-D vibrational echo decays at (from top to bottom) 80, 100, and 280 K. There are no anharmonic beats because of the very small spectral overlap of the 0–1 and 1–2 lines. The inset shows that the low temperature (100 K) 0–1 data decay as an exponential. (c) Frequency-selected vibrational echo decays (slices through the 2-D spectrum) at 280 K detected at the peaks of the 0–1 (squares) and 1–2 (circles) transitions. The decays at positive delays are virtually identical and non-exponential.

three temperatures (80, 100, and 280 K, top curve to bottom curve). Because the inhomogeneous broadening is small compared to the anharmonicity, no obvious anharmonic beats are observed in the 1-D data, even when the temperature is below the glass transition temperature (80 K data) [12,14]. Nonetheless, for positive delay times all of the terms R_1/R_2 and R_3 (Fig. 1a) contribute to the echo signals, and the decays reflect the combined dephasing dynamics of the 0–1 and 1–2 transitions. In the frequency-selected experiment (Fig. 5c), setting the detection wavelength at the peaks of the 0–1 and 1–2 transitions, yields the dephasing dynamics associated with R_1/R_2 and R_3 terms, respectively. At high temperature (e.g., 280 K, Fig. 5c), the vibrational echo decay profiles at positive times associated with R_1/R_2 (squares) and R_3 (circles) terms display strongly non-exponential behaviors that are virtually identical. This supports the assumption made above that the pure dephasing rates associated with 0–1 and 1–2 transitions are very similar, and the difference in the decays for the 0–1 and 1–2 transitions at low temperatures (Fig. 4) arises from difference in their lifetimes. At 280 K in 2-MTHF, the lifetime makes a negligible contribution to the vibrational echo decay (the lifetime of $v = 1$ level is ~ 16 ps at 280 K).

It is frequently assumed that a vibrational absorption line in a liquid at or near room temperature is homogeneously broadened and motionally narrowed because solvent dynamics are very fast at such elevated temperatures. In the motional narrowing limit, the spread in vibrational transition frequencies is averaged into a Lorentzian line (linear spectrum), and the vibrational echo decay is exponential [29–31]. The above argument is based on the assumption that there is a single time scale for solvent modulation of the vibrational transition frequency. The non-exponential decay observed at high temperatures in liquid 2-MTHF demonstrates that the simplified picture discussed above does not apply to this system in the liquid at 280 K. Instead, the solvent modulation of the vibrational transition frequency occurs on a variety of time scales [32]. The vibration is not completely homogeneously broadened nor is it in the inhomogeneous limit. Similar observations of vibrational transitions that are not completely

homogeneously broadened have been made with IR and Raman vibrational echo experiments previously [24,32]. Another interesting feature of this system is that the decay becomes exponential in the liquid near the glass transition temperature (86 K) and in the glass. The inset in Fig. 5b shows the 0–1 data taken at 100 K on a semi-log plot. The decay is not only much slower than at 280 K, but the decay is exponential, suggesting that solvent modulation time scales at this temperature are well separated in 'fast' and 'slow' components. The mechanism of the temperature dependence of the solvent fluctuation time scales and modulation magnitudes will be discussed in detail elsewhere [33].

Another feature of the vibrational echo decay data taken in 2-MTHF is that significant signals were observed in the negative time region (Fig. 5c). Such signals are due to the contributions from the R_7 and R_8 terms in Fig. 1. The signals at negative times are significantly larger than those observed in the PMMA solvent. The large negative time signals for RuTPPCOPy/2-MTHF are caused, in part, by the relatively narrow inhomogeneous CO stretching mode absorption line width in 2-MTHF compared to that in PMMA. Since R_7 and R_8 are non-rephasing terms, their contributions will be minimized when a large amount of inhomogeneity exists. Inspection of the vibrational echo signals at the two wavelengths (Fig. 5c) corresponding to the 0–1 (squares) and 1–2 (circles) transitions, shows that the signal at the 1–2 detection wavelength is larger in the negative time delay region than the 0–1 signal when the signals are matched at their peaks. This difference in amplitude is observed at a variety of temperatures. When the detection wavelength is close to the peak of the 0–1 transition, R_1, R_2, R_4, R_5, R_7 contribute to the total signal, and R_7 and the rising edges of the other four terms will contribute to the signal at negative time delay. When the detection wavelength is located at the peak of 1–2 transition, R_3, R_6 and R_8 contribute to the total signal, and R_8 and the rising edges of other two terms contribute to the signal at negative delays. At significant negative delay, the signal arises only from R_7 for the 0–1 detection wavelength and only from R_8 for the 1–2 detection wavelength. The mechanism responsible for the different signal amplitudes at negative delay times is unknown. Both the R_7 and R_8 terms involve 0–1 and 1–2 transitions to the same extent and should give equal contributions to the negative delay signals. In the harmonic approximation, the transition dipole matrix element for the 2–1 transition is $\sqrt{2}$ times of that for the 1–0 transition. At the signal level, (matrix element squared), the sum of R_1 and R_2 (or R_4 and R_5) will give the same amount of the signal as that of R_3 (or R_6). After normalization at the peak of the signal, the same amount of signal would be expected at both detection wavelengths at negative delay times. It is also worth noting that the negative time delay signals involve a 2–0 coherence. In principle, information on the decay of the 2–0 coherence can be obtained from analysis of the negative time delay signals.

4. Concluding remarks

Ultrafast infrared vibrational echo experiments inherently involve pulses with bandwidths that can exceed the vibrational anharmonicity of a particular transition and the differences between other vibrational transition splittings. Frequently, the information that is desired from a vibrational echo experiment is the dynamics of a particular two-state transition because two-level dynamics are most readily described theoretically. Comparison of the vibrational echo decays in Figs. 2 and 4 demonstrates that spectrally resolving the vibrational echo and detecting the signal at particular wavelengths can simplify the nature of the decays and provide the desired information.

Spectrally resolving the vibrational echo signal of the CO stretching mode of RuTPPCOPy permitted comparison of the vibrational echo decays (vibrational dephasing) of the 0–1 (fundamental) and the 1–2 transitions. At low temperatures, single exponential decays were observed in both solvents suggesting dynamical time scales (homogeneous and inhomgeneous broadening) are well separated. The 1–2 decay is faster than the 0–1 decay. Because population relaxation is a significant contribution to the vibrational echo decay at low temperatures, it was suggested that the dif-

ference in the decay rates is associated with a faster population relaxation from the second vibrational level than from the first level. At high temperature in 2-MTHF liquid, the decays, which are dominated by pure dephasing processes, are virtually identical and are non-exponential. The non-exponential decays in the high temperature liquid show that the dynamics cannot be described in terms of a motionally narrowed, totally homogeneously broadened absorption line produced by solvent modulation on a single time scale. Instead it suggests that solvent modulation of the vibrational transition frequency occurs on a variety of time scales, which cannot be well separated into homogeneous and inhomgeneous broadening. The temperature dependence of the vibrational dephasing of RuTPPCOPy in PMMA and 2-MTHF and the underlying dephasing mechanisms will be discussed in detail subsequently [33].

Acknowledgements

This work was supported by the National Institutes of Health (1R01-GM61137) and the National Science Foundation (DMR-0088942). KAM was partially supported by an Abbott Laboratories Stanford Graduate Fellowship.

References

[1] M.L. Horng, J.A. Gardecki, A. Papazyan, M. Maroncelli, J. Phys. Chem. 99 (1995) 17311.
[2] C. Rullière, Femtosecond Laser Pulses: Principles and Experiments, Springer, Berlin, 1998.
[3] D.S. Larsen, K. Ohta, Q.H. Xu, M. Cyrier, G.R. Fleming, J. Chem. Phys. 114 (2001) 8008.
[4] L.D. Book, N.F. Scherer, J. Chem. Phys. 111 (1999) 792.
[5] K. Ohta, D.S. Larsen, M. Yang, G.R. Fleming, J. Chem. Phys. 114 (2001) 8020.
[6] D. Zimdars, A. Tokmakoff, S. Chen, S.R. Greenfield, M.D. Fayer, T.I. Smith, H.A. Schwettman, Phys. Rev. Lett. 70 (1993) 2718.
[7] A. Tokmakoff, M.D. Fayer, J. Chem. Phys. 102 (1995) 2810.
[8] K.D. Rector, M.D. Fayer, Int. Rev. Phys. Chem. 17 (1998) 261.
[9] K.D. Rector, M.D. Fayer, J. Chem. Phys. 108 (1998) 1794.
[10] M.C. Asplund, M. Lim, R.M. Hochstrasser, Chem. Phys. Lett. 323 (2000) 269.
[11] M.T. Zanni, M.C. Asplund, R.M. Hochstrasser, J. Chem. Phys. 114 (2001) 4579.
[12] D.E. Thompson, K.A. Merchant, M.D. Fayer, J. Chem. Phys. 115 (2001) 317.
[13] K.A. Merchant, D.E. Thompson, M.D. Fayer, Phys. Rev. Lett. 86 (2001) 3899.
[14] K.A. Merchant, D.E. Thompson, M.D. Fayer, Phys. Rev. A 65 (2002) 23817.
[15] O. Golonzka, M. Khalil, N. Demirdoven, A. Tokmakoff, Phys. Rev. Lett. 86 (2001) 2154.
[16] N. Demirdoven, M. Khalil, O. Golonzka, A. Tokmakoff, J. Phys. Chem. A 105 (2001) 8030.
[17] M. Khalil, A. Tokmakoff, Chem. Phys. 266 (2001) 213.
[18] C.W. Rella, K.D. Rector, A.S. Kwok, J.R. Hill, H.A. Schwettman, D.D. Dlott, M.D. Fayer, J. Phys. Chem. 100 (1996) 15620.
[19] K.D. Rector, J.R. Engholm, C.W. Rella, J.R. Hill, D.D. Dlott, M.D. Fayer, J. Phys. Chem. A. 103 (1999) 2381.
[20] K.D. Rector, J. Jiang, M. Berg, M.D. Fayer, J. Phys. Chem. B 105 (2001) 1081.
[21] K.D. Rector, C.W. Rella, A.S. Kwok, J.R. Hill, S.G. Sligar, E.Y.P. Chien, D.D. Dlott, M.D. Fayer, J. Phys. Chem. B. 101 (1997) 1468.
[22] M.C. Asplund, M.T. Zanni, R.M. Hochstrasser, Proc. Natl. Acad. Sci. USA 97 (2000) 8219.
[23] M.D. Fayer, Ann. Rev. Phys. Chem. 52 (2001) 315.
[24] A. Tokmakoff, M.D. Fayer, J. Chem. Phys. 103 (1995) 2810.
[25] A. Tokmakoff, A.S. Kwok, R.S. Urdahl, R.S. Francis, M.D. Fayer, Chem. Phys. Lett. 234 (1995) 289.
[26] K.D. Rector, A.S. Kwok, C. Ferrante, A. Tokmakoff, C.W. Rella, M.D. Fayer, J. Chem. Phys. 106 (1997) 10027.
[27] S. Mukamel, Principles of Nonlinear Optical Spectroscopy, Oxford University Press, New York, 1995.
[28] K.A. Merchant, D.E. Thompson, Q.-H. Xu, R.F. Loring, M.D. Fayer, Biophys. J., 2002, accepted.
[29] R. Kubo, in: D. Ter Haar (Ed.), Fluctuation, Relaxation and Resonance in Magnetic Systems, Oliver and Boyd, London, 1961.
[30] M.A. Berg, K.D. Rector, M.D. Fayer, J. Chem. Phys. 113 (2000) 3233.
[31] T.C. Farrar, D.E. Becker, Pulse and Fourier Transform NMR, Academic Press, New York, 1971.
[32] M.A. Berg, H.W. Hubble, Chem. Phys. 233 (1998) 257.
[33] Q.-H. Xu, M.D. Fayer, J. Chem. Phys., 2002, submitted.